EXTRACTION OF SEMI-URBAN LANDSCAPES WITH REMOTELY SENSED DATA USING MAXIMUM LIKELIHOOD CLASSIFICATION TECHNIQUE

G. S. Sinchana*[1], A. L. Choodarathnakara[2], M. N. Rashmi[3], Arpitha G. A.[4] and Shashikala N.[5]

[1, 4] *Research Scholar, Dept. of E&C Engineering, Government Engineering College, Kushalnagar 571234.*
EMAIL ID: msruas.sinchanags@gmail.com, arpithaga6@gmail.com
[2] *Associate Professor, Dept. of E&C Engineering, Government Engineering College. Karwar 581345*
EMAIL ID: choodarathnakara@gmail.com
[3] *Lecturer, Dept. of Electrical and Electronics Engineering,*
Government Polytechnic, Mirle – 571603
EMAIL ID: rmn208@gmail.com
[5] *Lecturer, Dept. of Electrical and Electronics Engineering,*
Government Polytechnic, K.R. Pete-571426
EMAIL ID: shashi.jan28@gmail.com

Abstract: A geospatial technique called remote sensing includes seeing and interpreting electromagnetic radiation that is emitted or reflected from surface of the Earth without making direct physical contact. It is crucial to identify and keep track of the physical traits of various ecosystems, including those in terrestrial, aerated, and aquatic environments. The categorization of Land Use and Land Cover (LU/LC) using remotely sensed data is an important study field in remote sensing. The Somvarpet taluk in Kodagu District is used for mapping and detecting LU/LC patterns. The LU/LC thematic map classification is performed on LANDSAT-8 satellite images from the years 2017–18 using Maximum Likelihood Classification (MLC) technique. The experiment was performed on five distinct training sample size as 100, 200, 300, 400, and 500 and examined semi-urban features using Panchromatic data. For these training sample sizes, the total classification accuracy achieved was 69.28%, 72.86%, 81.90%, 84.44%, and 90.80%, respectively. Additionally, for these training sample sizes, the corresponding Kappa Statistics were 0.5979, 0.6042, 0.7249, 0.7493, and 0.8510. Future studies can concentrate on enhancing urban feature classification accuracy and in-depth investigation of the variables influencing classification performance.

Keywords: Remote Sensing, Land Use/Land Cover, Maximum Likelihood Classification, Semiurban region

Introduction

Land use and land cover (LU/LC) are two distinct terms, that are frequently used synonymously. The distribution of flora, water, soil and other physical aspects of land and along with the human activity, such as settlements, are all considered to be part of land cover, which used to describe the physical properties of the earth's surface.

An analysis was performed in the Egyptian Lake Maryut to distinguish the best strategy for restoring the changes. The outcomes specified that severe LC changes occurred in different LC especially in the last few years that may be due to political and socio-economic problems. Finally, a modern method based on the Delphi technique was applied to select the best restoration alternative for restoring the Lake Maryut [2]. LC maps are significant tools for quantifying the

human footprint on the atmosphere and facilitate reporting and accounting to international agreements addressing the sustainable development goals [7]. While LU refers to how humans and their habitat have used land, typically with a focus on the land's functional role for economic activity [4]. One of the most appealing methods for effectively obtaining LC data is remotely sensed (RS) image classification. Unsupervised and supervised classification are the two general

categories into which RS image classification falls. The most common application of unsupervised classification algorithms is to comprehend the spectral properties of land cover classes. Based on probability theory, the Maximum Likelihood Classifier (MLC) operates. When training the data, MLC makes the assumption that the statistics for each class in each band are Gaussian distributed [12].

Using MLC and the Random Forests (RF) method, three distinct study sites comprising extremely diverse landscapes were highlighted for novel research on completely automatic and cost-effective LC classification method. The overall agreement of the new automatic classification method is 90.0%, 89.5%, and 89.9% for the study areas of Rijeka, Zagreb, and Sarajevo, respectively, according to the results. The overall agreement always falls between the MLC method's (88.1%, 88.9%, and 86.7%) and the RF method's (91.7%, 90.4%, and 90.2%) overall agreement. These findings validate the ease of use of this novel automatic, economical and precise land cover classification technique for a wide range of remote sensing uses [19].

In contrast to Naive Bayes (NB), Random Forest (RF), Multilayer Perceptron (MLP) and Support Vector Machine (SVM), the author found, Decision tree (DT) J48 classifier was the effective technique for differentiating between urban regions and natural vegetation cover [13]. Using Sentinel-2 satellite images, this study investigates the effects of five distinct atmospheric correction processing methods on the accuracy of land cover classification. For all twelve days, SVM classification yielded the best overall result when accounting for atmospheric corrections. S2AC, with a median value of 96.54%, is the best atmospheric adjustment for classification with SVM using radiometric indices, whereas STDSREF, with a median value of 96.83%, is the best correction without radiometric indices [17]. In this research, an automatic technique for classifying land cover in the north of China was proposed utilizing time-series Landsat data on the GEE cloud-based platform. Two types of spectral-temporal features were employed as input features to the RF classifier for land-cover classification. These features were created using all available Landsat Thematic Mapper (TM) and Enhanced Thematic Mapper Plus (ETM+) data from the year 2010 ± 1. According to the results, the monthly features fared better than the percentile features, with an average OA of 80% as opposed to 77%. Consequently, the suggested approach, which is based on the GEE cloud-based platform, can automatically produce accurate land-cover mapping, which holds promise for regional and global land-cover mapping [5]. This study recommended that the continuous Landsat classification via random forest classifier could be effective in monitoring the long-term dynamics of LULC changes and provide crucial information and data for the understanding of the driving forces of LULC change, environmental impact assessment and ecological protection planning in large-scale mining areas [14].

In this study, it provides a reference for the extraction of LUCC information in case of dryland regions with oasis-desert mosaic landscapes by associating the performances with machine

learning models in Dengkou Oasis, China. Hence the maximum overall accuracy formed by the ANN was 97.16%, which was closely followed by the RF (96.92%), SVM (96.20%) and KNN (93.98%). As a further recommendations, the elevation and some spectral indices such as NDVI, MSAVI2 and MNDWI can be applied as a variables to improve the overall accuracy [9]. The Landsat 8 satellite of Operational Land Imager (OLI) image (path/row 139/43) downloaded from the USGS website have been employed to map the LULC using different machine-learning algorithms. Experimental outcomes of Kappa coefficient show that all the classifiers have a similar accuracy level with minor variation, but the RF algorithm has the highest accuracy of 0.89 and the Mahalanobis distance (MD) algorithm (parametric classifier) has the least accuracy of 0.8215.

LU/LC dynamic variations were investigated using LISS-III data for Harangi catchment for years 2007, 2010, and 2013. Three classification techniques—Parallelepiped, Minimum Distance to Mean, and Maximum Likelihood—were compared. The primary causes of the growth in plantations and urban areas at the expense of the decline in forest regions are urbanization and agricultural activity [3].

A deforestation and LULC changes dynamics in west Singhbhum for the period 1997-2017 using supervised classification of maximum likelihood algorithm and post-classification CD technique was conducted for the last 20 years with the help of Landsat multi-spectral data. The result reveals that agriculture is the solitary class that has augmented significantly and showed that spare vegetation had a major loss due to the increased demand of the agricultural land and growth in mining and settlement area [1].

A study on the position of LULC changes and key drivers of change for the last 30 years through a combination of RS and GIS with the surveying of the local community understanding of LULC patterns and drivers in the Gubalafto district, North-eastern Ethiopia was assessed for three study periods: Landsat 5 TM 1986 and Landsat 7 ETM + 2000. The outcomes provided that the grazing land in 1986 was about 11.1% of study area and it had decreased to 5.7% in 2016 [4].

The study demonstrates the spatio-temporal dynamics of land use/cover of Hawalbagh block of district Almora, Uttarakhand, India using LTM at a resolution of 30m of 1990 and 2010 were used. The satellite data covering study area were obtained from global land cover facility (GLCF) (http://glcfapp.glcf.umd.edu:8080/esdi/) and earth explorer site (http://earthexplorer.usgs.gov/). The results indicated that during the last two decades, vegetation as well as built-up land have been increased by 3.51% (9.39 km2) and 3.55% (9.48 km2) while agriculture, barren land, and water body have decreased by 1.52% (4.06 km2), 5.46% (14.59 km2) and 0.08% (0.22 km2), respectively [6].

To examine LCLU changes and assess the utility of the approach for monitoring human-induced changes, an innovative "dense stack" approach of image classification approach with extremely cloudy, multi-temporal Landsat 7 ETM+ imagery map within southern Ghana for circa 2000 and circa 2010 was considered8. The results indicate that extreme land cover variations has happened in agricultural (36.2%) (especially in tea gardens), urban (117%), pasture (-72.8%) and forestry (-12.8%) areas have experienced in the region between 1976 and 2000 [11]. ALOS-2 PALSAR L-band dual-polarization (HH and HV) SAR data and Landsat-8 optical imagery for land cover classification in a portion of Tehsil Chichawatni in district Sahiwal, Punjab province,

Pakistan was examined. Where SAR classified output gave accuracy of 93.15% and the Landsat8 classified map accuracy was 91.34%, while the Kappa coefficient for SAR and Landsat-8 classified images is 0.92 and 0.89, respectively [10].

This paper presents an unsupervised approach that extracts reliable labelled units from outdated maps to update them using time series (TS) of recent multispectral (MS) images. the source of the map is unknown and may be different from RS data. The experimental results obtained updating the 2012 Corine Land Cover (CLC) and the GlobLand30 in Trentino Alto Adige (Italy) achieved 93.2% and 93.3% overall accuracy (OA) on the validation data set [16].

From current world-wide coverage of open-access for geospatial datasets, it was highlighted that object-based LULC classification accuracy observed to be higher. Auxiliary features in other models raised the median OA by 6.1 to 16.5 percentage points, compared to the baseline model's 60.7%. Elevation was the most significant auxiliary parameter, followed by the temporal range and slope degree of the Enhanced Vegetation Index, in a model that included all features and produced the best overall analysis [18]. The current paper is organized as follows: Section I includes introduction to remote sensing, LU/LC concepts and its applications. Section II provides the details of study area used in this study. Section III describes the proposed methodology. In section IV the experimental results are presented to analyse Semi urban features of Panchromatic data. Section V presents some concluding remarks.

STUDY AREA

The study area considered for our work is the semi-urban area of Somwarpet region as shown in Fig 1. It is situated in Kodagu district, Karnataka state, India. Its geographical coordinates are 12.5943° North, 75.8505° East and its original name (with diacritics) is Somvarpet. It has an average elevation of 1,130 meters.
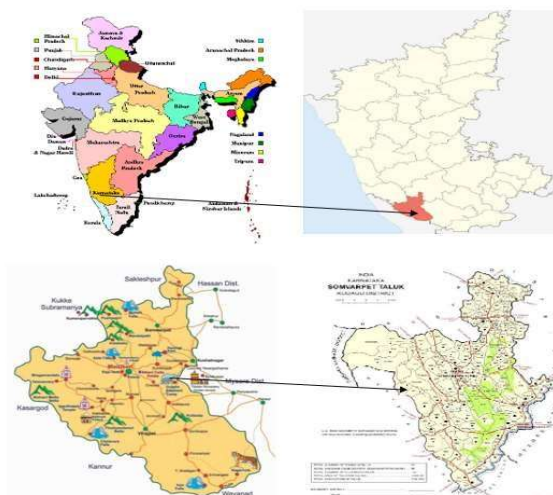
Fig 1. Study area: Somwarpet, Kodagu, Karnataka, India.

Proposed Methodology

The proposed Parametric and Non-Parametric algorithm consisting of the following steps:

Step 1: Start

Step 2: Data collection using LANDSAT-8 and Google Earth Data.

Step 3: Pre-processing (subsetting, geocorrection, fusion) of Data using ERDAS Imagine version 9.2.

Step 4: Detection of Semi urban features using Hierarchy Level-1 (CHL-1).

Step 5: To study the CHL-I Semi urban features using Panchromatic (layer 8)

Step 6:   Five sets of Training samples were taken for 7 different Semi urban features in both panchromatic and fused Data.

Step 7: Classification using supervised Maximum Likelihood classification algorithm.

Step 8: 1/3 rd of training samples are taken as the validation set and assessment of accuracy was accomplished for this validation set.

Step 9: Comparison between overall accuracy v/s training sample, overall kappa v/s   training sample and different LULC features.

Step 10:   Comparison of Semi urban Features in percentage.

Step 11: Performance analysis of supervised Classifier for panchromatic data were performed.

Step 12:   End
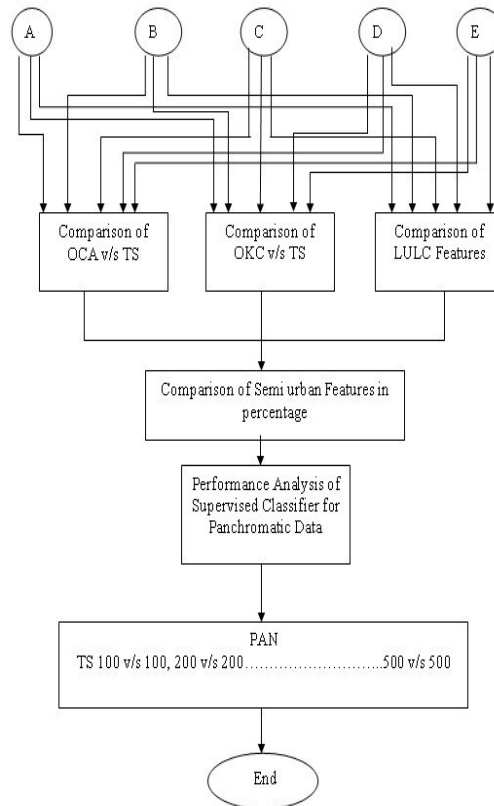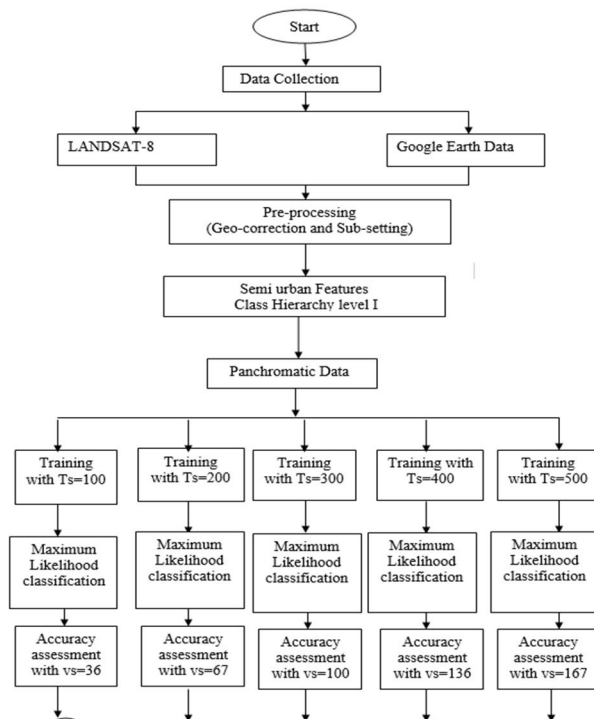
Fig 2. Performance assessment of Maximum Likelihood classifier.

Result Analysis of Maximum Likelihood Technique for PAN Data

Fig 3. Shows the input panchromatic image
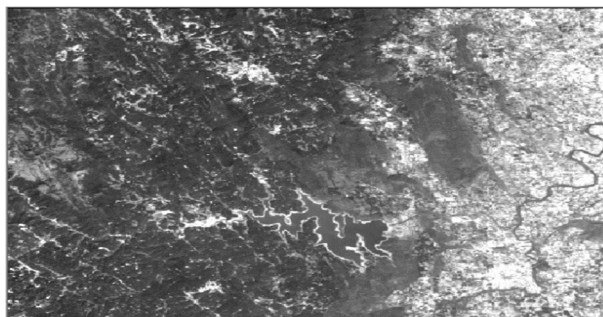
Fig 3. Input panchromatic image

Maximum Likelihood Technique for PAN Data Experimental results for various Training Set and Validation Set
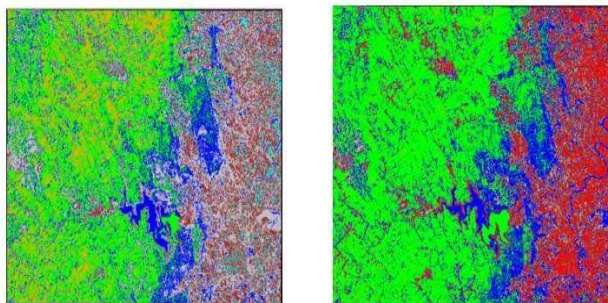
Fig 4. MLC Classified Image using 100 and 200 training samples for pan data.
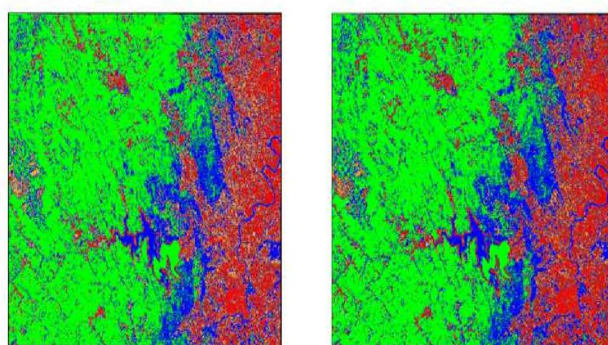
Fig 5. MLC Classified image of 300 and 400 training samples for panchromatic data.
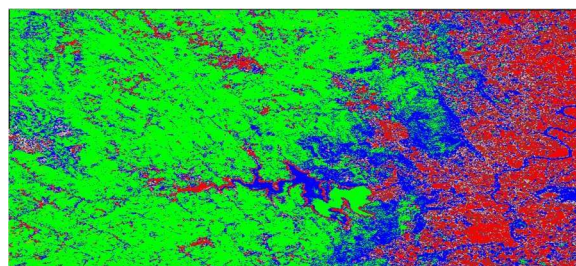
Fig 6. MLC Classified image of 500 training samples for panchromatic data

For each class, 100, 200, 300, 400 and 500 training set and validation set of 35, 70, 100, 135 and 170 is performed for extraction of semi-urban features as shown in the Fig 4, 5 and 6.

Table 2. Error Matrix and Kappa Values obtained for MLC Supervised Classification for seven classes with 100 training samples and 35 validations set.

Reference Pixels

Class	1	2	3	4	5	6	7	RT	UA
1	1	3	0	2	1	1	0	8	12.5%
2	0	14	0	0	0	0	0	14	100%
3	0	0	3	1	0	0	0	4	75%
4	0	0	0	4	0	0	0	4	100%
5	0	0	0	0	2	0	0	2	100%
6	0	4	0	0	0	0	0	4	0%
7	0	0	0	0	0	0	2	2	100%
CT	1	21	3	7	3	1	2	38	
PA	100%	66.6%	100%	57.14%	66.6%	0%	100%		
Kappa	0.1020	1.0000	0.7292	1.0000	1.0000	-0.0263	1.0000		

Legend: 1=Water bodies, 2=Forest, 3=Wasteland, 4=Agriculture, 5=Wetland, 6=Grassland, 7=Built up, CT= Column Total, RT=Row Total, UA= User Accuracy, PA= Producer Accuracy.

Table. 3. Error Matrix for 200 training samples and 70 validity set.

Class	1	2	3	4	5	6	7	RT	UA
1	30	0	1	0	0	0	0	31	96.77%
2	7	5	1	1	2	0	0	16	31.25%
3	1	0	2	0	1	0	0	4	50%
4	1	0	0	0	1	0	0	2	0%
5	0	0	0	0	12	0	0	12	100%
6	0	0	0	0	3	1	0	4	25%
7	0	0	0	0	0	0	1	1	100%
CT	39	5	4	1	19	1	1	70	
PA	76.92%	100%	50%	0%	63.13%	100%	100%		
Kappa	0.9272	0.2596	0.467	0.0145	1.0000	0.2391	1.0000		

Legend: 1=Forest, 2=Water bodies, 3=wasteland, 4=Grassland, 5=Agriculture, 6=Built up, 7=wetland, CT= Column Total, RT=Row Total, UA= User Accuracy, PA= Producer Accuracy.

Table 4. Error Matrix for 300 training samples and 100 validity set.

Class	1	2	3	4	5	6	7	RT	UA	Kappa
1	5	2	0	0	0	0	0	7	71.43%	0.7000
2	0	4	0	0	0	0	0	4	100%	1.0000
3	0	0	3	1	1	0	0	5	60%	0.5882
4	0	0	0	7	0	0	0	7	100%	1.0000
5	0	0	0	0	12	0	0	12	100%	1.0000
6	0	0	0	0	0	54	1	55	98.18%	0.9556
7	0	3	0	0	3	8	1	15	6.67%	0.0485
CT	5	9	3	8	16	62	2	105		
PA	100%	44.4%	100%	87.5%	75%	87.1%	50%			

Legend: 1=Grassland, 2=Wasteland, 3=built up, 4=Wetland, 5=Agriculture, 6=Forest, 7=Water bodies, CT= Column Total, RT=Row Total, UA= User Accuracy, PA= Producer Accuracy.

Table 5. Error Matrix for 400 training samples and 135 validity set

Class	1	2	3	4	5	6	7	RT	UA	Kappa
1	7	0	0	0	1	0	0	8	87.50%	0.8682
2	0	3	0	0	0	0	0	3	100%	1.0000
3	0	0	7	0	0	0	0	7	100%	1.0000
4	0	0	0	7	2	0	0	9	77.7%	0.7656
5	0	1	1	0	12	1	1	16	75%	0.7091
6	0	1	0	0	4	2	9	16	12.5%	0.1051
7	0	0	0	0	0	0	75	75	100%	1.0000
CT	7	5	8	7	19	3	85	135		
PA	100%	60%	87.5%	100%	63.16%	66.67%	88.24%			

Legend: 1=Grassland, 2=wasteland, 3=Wetland, 4=Built up, 5=Agriculture, 6=Water bodies, 7=Forest, CT= Column Total, RT=Row Total, UA= User Accuracy, PA= Producer Accuracy.

Table 6. Error Matrix for 500 training samples and 170 validity set

Class	1	2	3	4	5	6	7	RT	UA	Kappa
1	8	0	0	0	0	0	0	8	100%	1.0000
2	0	2	0	0	0	0	0	2	100%	1.0000
3	1	0	22	2	0	0	0	25	88%	0.8589
4	0	0	0	5	0	0	0	5	100%	1.0000
5	0	0	2	2	8	0	0	12	66.67%	0.6506
6	0	0	0	0	0	99	0	99	100%	1.0000
7	0	1	2	0	0	6	14	23	60.87%	0.5745
CT	9	3	26	9	8	105	14	172		
PA	88.89%	66.67%	84.62%	55.56%	100%	94.29%	100%			

Legend: 1=Wasteland, 2=Grassland, 3=Agriculture, 4=Wetland, 5=Built up, 6=Forest, 7=Water bodies, CT= Column Total, RT=Row Total, UA= User Accuracy, PA= Producer Accuracy

From Table 2, 3, 4, 5 and 6, it interprets that for 100 training samples, the total study area has been assigned for panchromatic as 1.54% of unclassified land, 3.714% of Wetland, 15.04% of Water, 33.34% of Forest, 22.67% of Wasteland, 13.18% of Agriculture, 15.93% of Grassland, 0.6686% of Built-up area respectively. Overall Classification Accuracy = 69.28%; Overall Kappa Statistics = 0.5979. For 200 training samples, the total study area has been assigned for panchromatic data as 1.54% of unclassified land, 47.58% of Forest, 20.22% of Water, 5.41% of Wasteland,3.61% of Grassland, 15.1132% of Agriculture, 6.3345% of Built up,0.1695% of Wetland respectively. Overall Classification Accuracy = 72.86%; Overall Kappa Statistics = 0.6042. For 300 training samples, the total study area has been assigned for panchromatic data as 1.54% of unclassified land, 7.435% of Grassland, 3.94% of Wasteland, 5.505% of Built up, 0.0923% of Wetland, 12.933% of Agriculture, 20.31% of Water, 48.24% of Forest respectively. Overall Classification Accuracy = 81.90%; Overall Kappa Statistics = 0.7249. For 400 training samples, the total study area has been assigned for panchromatic data as 1.54% of unclassified land, 7.065% of Grassland, 1.53% of Wasteland, 5.77% of Built up, 14.01% of Agriculture, 0.066% of Wetland, 48.25% of Forest, 21.77% of Water, respectively. Overall Classification Accuracy = 84.44%; Overall Kappa Statistics = 0.7493. For 500 training samples, the total study area has been assigned for panchromatic data as 1.54% of unclassified land, 1.907% of Grassland, 4.75% of Wasteland, 0.021% of Wetland, 13.28% of Agriculture, 6.722% of Built up, 48.826% of

Water, 38.82% of Forest respectively. Overall Classification Accuracy = 90.80%; Overall Kappa Statistics =0.8510.

Comparison of OKS v/s TS
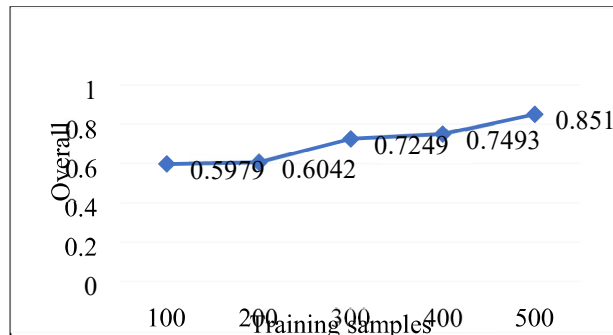
Fig 7. Comparison of overall Kappa statistics v/s training samples

Fig 7. shows comparison of overall kappa statistics v/s training samples. Kappa Statistic is based on the difference between the actual agreement in confusion matrix (i.e., the agreement between the remotely sensed classification and reference data is indicated by the major diagonal) and the chance agreement, which is indicated by the row and column totals (i.e., marginals). For training set 100 obtained overall kappa statistics is 0.5979. Similarly, for training set 200, the obtained overall kappa statistics is 0.6042. For the training set of 300, the obtained overall kappa statistics is 0.7249. For the training sets of 400 and 500, the obtained overall kappa statistics is 0.7493 and 0.851 respectively. This comparison of overall kappa statistics v/s training samples was obtained for LANDSAT 8 panchromatic image. As the training sets were increased, the overall kappa statistics also increased.

LULC Features with TS=100, 200, 300, 400 and 500

Fig 8, 10, 12, 14 and 16. shows the Comparison of Area in pixels and acres v/s Semi urban Features. From the figure 8, it was noticed that the total area in pixels has been classified as 44253 of unclassified land, 106712 of wetland, 432206 of water, 957792 of forest, 378775 of agriculture land, 651350 of waste land, 282769 of grass land and 19209 of Built up area. Along with forest, water body are also have been mainly classified. Correspondingly, along with Built up, wetland has been least classified.
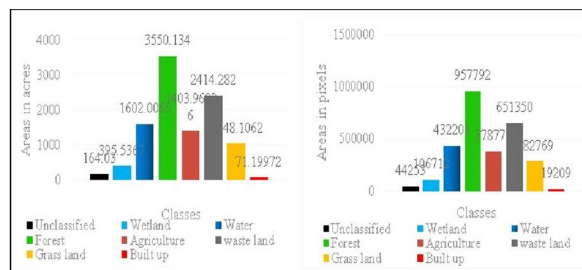
Fig 8. Comparision of LULC Features v/s Area in pixels and acres.
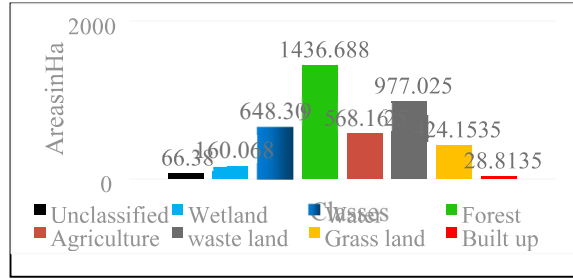
Fig 9. Comparision of LULC Features v/s Area in Ha.
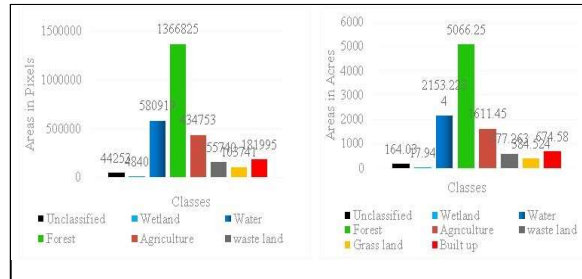
Fig 10. Comparison of LULC Features v/s Area in pixels and acres.
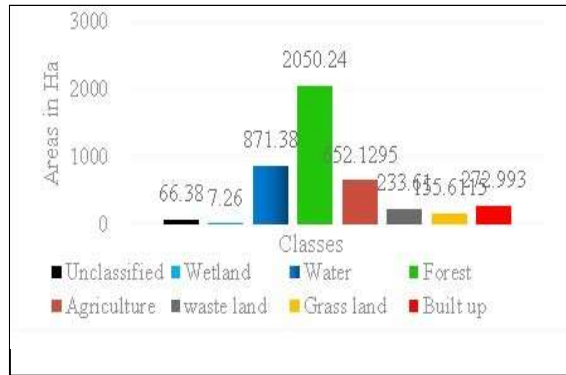
Fig 11. Comparison of LULC Features v/s Area in Ha.
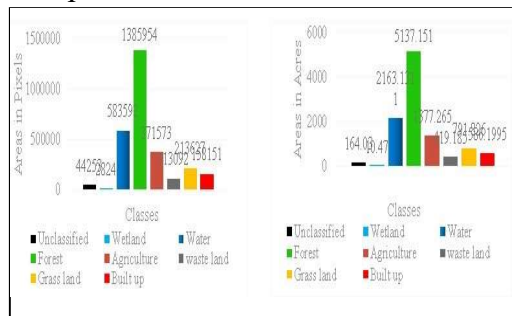
Fig 12. Comparison of LULC Features v/s Area in pixels and acres.
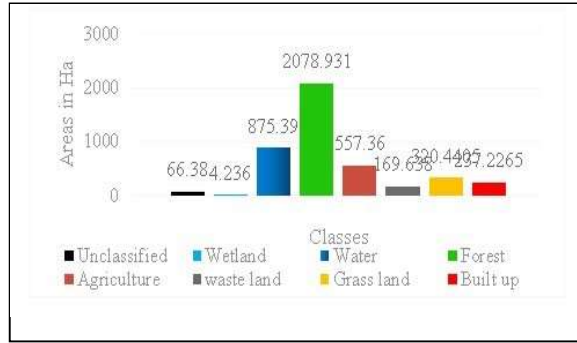
Fig 13. Comparison of LULC Features v/s Area in Ha.
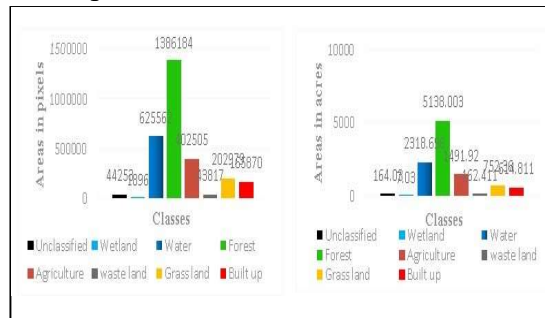
Fig 14. Comparison of LULC Features v/s Area in pixels and acres.
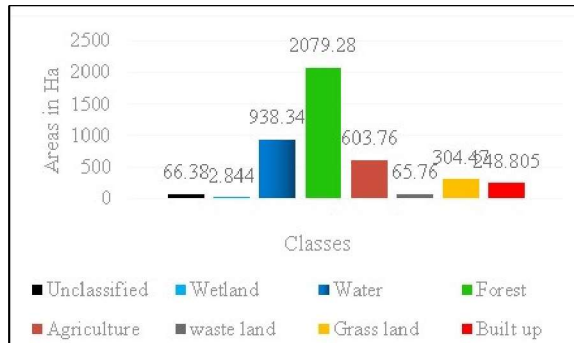
Fig 15. Comparison of LULC Features v/s Area in Ha.
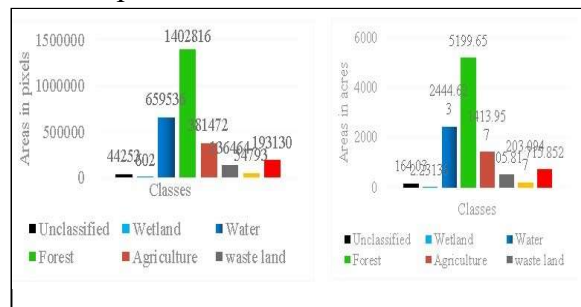
Fig 16. Comparison of LULC Features v/s Area in pixels and acres.
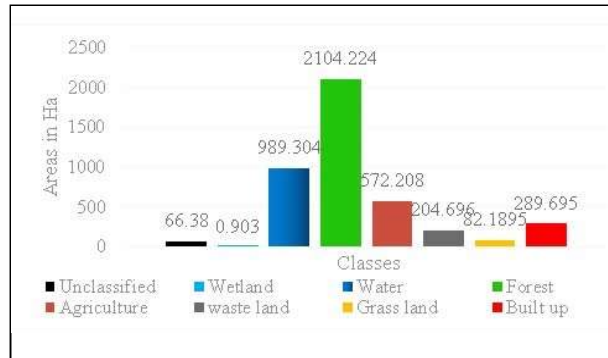
Fig 17. Comparison of LULC Features v/s Area in Ha.

The total area in acres has been classified as 164.03 of unclassified land, 395.5367 of wetland, 1602.0066 of water, 3550.134 of forest, 1403.9602 of agriculture land, 2414.282 of waste land, 1048.106 of grass land and 71.199 of Built up area. Along with forest, water body are also has been mainly classified. Correspondingly, along with built up, wetland has been least classified. Similarly, the total study area in pixels and acres interpretation have been assigned for panchromatic data for the Fig 10, 12, 14 and 16.

Fig 9, 11, 13, 15 and 17. shows the Comparison of Area in pixels, acres and Ha v/s Semi urban Features. From the Fig 9, it was noticed that the total study area are assigned in Ha as 66.38 of unclassified land, 160.068 of wetland, 648.309 of water, 1436.668 of forest, 568.1625 of agriculture land, 977.025 of waste land, 424.1535 of grass land and 28.8135 of Built up area. Along with forest, water body are also has been mainly classified. Correspondingly, along with Built up, wetland has been least classified. Similarly, the total area interpretation has been classified for panchromatic data for the Fig 11, 13, 15 and 17.

Conclusion

The chief objective of this paper was to study the area for semi urban feature classification purpose using Maximum likelihood classification. The approaches used here are to solve the existing problem using MLC and it tracks the amount of Land use Land cover using the remote sensing techniques by extracting the local features using MLC. Comparing and classifying image to detect the LU/LC changes. The experimentation is conducted on image dataset developed for classification using Google Earth Images. The implementation of the proposed methodology is carried out using ERDAS version 9.2 is an Image processing software to study the Semi urban features using Panchromatic (layer 8) data. Semi urban features of Panchromatic data were collected and analyzed for five training samples, for 100 training samples, overall classification accuracy of 69.28% and Kappa Statistics of 0.5979 was obtained; For 200 training samples, Overall Classification Accuracy of 72.86% and Kappa Statistics of 0.6042 was obtained. For 300 training samples, Overall Classification Accuracy of 81.90% and Kappa Statistics of 0.7249 was obtained. For 400 training samples, Overall Classification Accuracy of 84.44% and Kappa Statistics of 0.7493 was obtained; For 500 training samples, Overall Classification Accuracy of 90.80% and Kappa Statistics of 0.8510 was obtained. Maximum likelihood supervised classification can be performed for better classification accuracy, and it provides a better

understanding of semi-urban features for urban planning at Somwarpet taluk. Improved classification accuracy over urban features and Important issues affecting classification performance are analyzed for future research.

Acknowledgements

Author contributions

Sinchana G. S. and Choodarathnakara A. L Conceptualization, Methodology, Data curation, Writing-Original draft preparation, Software, Validation., Arpitha G. A. , Rashmi M. N and Shashikala N.: Visualization, Investigation, Writing-Reviewing and Editing.

References

[1] J. Jinju, N. Santhi, K. Ramar, & B. S. Bama, "Spatial frequency discrete wavelet transforms image fusion technique for remote sensing applications," Engineering Science and Technology, vol. 22, no. 3, pp. 715-726, 2019.

[2] D. Kaimaris, P. Patias, G. Mallinis, & C. Georgiadis, "Data Fusion of Scanned Black and White Aerial Photographs with Multispectral Satellite Images," Sci., vol. 2, no. 2, pp. 29, 2020.

[3] Y. Quan, Y. Tong, W. Feng, G. Dauphin, W. Huang, & M. Xing, "A Novel Image Fusion Method of Multi-Spectral and SAR Images for Land Cover Classification," Remote Sensing, vol. 12, no. 22, pp. 3801, 2020.

[4] D. Mishra, & B. Palkar, "Image fusion techniques: a review," International Journal of Computer Applications, vol. 130, no. 9, pp. 7-13, 2015.

[5] Y. Zhang, "Understanding image fusion. Photogramm. Eng.," Remote Sens., vol. 70, no. 6, pp. 657-661, 2004.

[6] X. Wei, N. B. Chang, & K. Bai, "A Comparative Assessment of Multisensory Data Merging and Fusion Algorithms for High-Resolution Surface Reflectance Data," IEEE Journal of Selected Topics in Applied Earth Observations and Remote Sensing, vol. 13, pp. 4044-4059, 2020.

[7] J. Fortuna, H. Martens, & T. A. Johansen, "Multivariate image fusion: A pipeline for hyperspectral data enhancement," Chemometrics and Intelligent Laboratory Systems, vol. 205, pp. 104 - 097, 2020.

[8] M. Ghahremani, Y. Liu, P. Yuen, & A. Behera, "Remote sensing image fusion via compressive sensing," ISPRS journal of photogrammetry and remote sensing, vol. 152, pp. 34-48, 2019.

[9] W. Li, R. Dong, H. Fu, J. Wang, L. Yu, & P. Gong, "Integrating Google Earth imagery with Landsat data to improve 30-m resolution land cover mapping," Remote Sensing of Environment, vol. 237, pp. 111 - 563, 2020.

[10]   Y. Peng, W. Li, X. Luo, J. Du, Y. Gan, & X. Gao, "Integrated fusion framework based on semicoupled sparse tensor factorization for spatio-temporal–spectral fusion of remote sensing images," Information Fusion, vol. 65, pp. 21-36.

[11]   K. Rangzan, M. Kabolizadeh, D. Karimi, & S. Zareie, "Supervised cross-fusion method: a new triplet approach to fuse thermal, radar, and optical satellite data for land use classification," Environmental monitoring and assessment, vol. 191, no. 8, pp. 481, 2019.

[12]   E. Shah, P. Jaya prasad, & M. E. James, "Image Fusion of SAR and Optical Images for Identifying Antarctic Ice Features," Journal of the Indian Society of Remote Sensing, vol. 47, no. 12, pp. 2113-2127, 2019.

[13]   Z. Shao, J. Cai, P. Fu, L. Hu, & T. Liu, "Deep learning-based fusion of Landsat-8 and Sentinel-2 images for a harmonized surface reflectance product," Remote Sensing of Environment, vol. 235, pp. 111425, 2019.

[14]   J. Useya, & S. Chen, "Comparative Performance Evaluation of Pixel-Level and DecisionLevel Data Fusion of Landsat 8 OLI, Landsat 7 ETM+ and Sentinel-2 MSI for Crop Ensemble Classification," IEEE Journal of Selected Topics in Applied Earth Observations and Remote Sensing, vol. 11, no. 11, pp. 4441-4451, 2018.

[15]   H. Wang, E. Skau, H. Krim, & G. Cervone, "Fusing heterogeneous data: A case for remote sensing and social media," IEEE Transactions on Geoscience and Remote Sensing, vol. 56, no. 12, pp. 6956-6968, 2018.

[16]   H. Wu, S. Zhao, J. Zhang, & C. Lu, "Remote sensing image sharpening by integrating multispectral image super-resolution and convolutional sparse representation fusion," IEEE Access, vol. 7, pp. 46562-46574, 2019.

[17]   S. Wu, & H. Chen, "Smart city oriented remote sensing image fusion methods based on convolution sampling and spatial transformation," Computer Communications, 2020.

[18]   Y. Yang, H. Lu, S. Huang, & W. Tu, "Remote Sensing Image Fusion Based on Fuzzy Logic and Salience Measure," IEEE Geoscience and Remote Sensing Letters, 2019.

[19]   F. Ye, X. Li, & X. Zhang, "FusionCNN: a remote sensing image fusion algorithm based on deep convolutional neural networks," Multimedia Tools and Applications, vol. 78, no. 11, pp. 14683-14703, 2019.

[20]   N. Yokoya, P. Ghamisi, J. Xia, S. Sukhanov, R. Heremans, I. Tankoyeu, & D. Tuia, "Open data for global multimodal land use classification: Outcome of the 2017 IEEE GRSS Data Fusion Contest," IEEE Journal of Selected Topics in Applied Earth Observations and Remote Sensing, vol. 11, no. 5, pp. 1363-1377, 2018.